
R.G. Cherkez, M.V. Maksymuk, P.P. Fenyak

Institute of Thermoelectricity of the NAS and MES Ukraine,
1, Nauky Str., Chernivtsi, 58029, Ukraine

DESIGN OF THERMOELECTRIC PERMEABLE STRUCTURES BASED ON *Mg* AND *Mn* SILICIDES

Results of computer design of permeable thermoelements based on Mg and Mn silicides are presented. Optimal concentrations of doping impurities for such materials and optimal thermophysical parameters whereby maximum thermodynamic efficiency of permeable thermoelements is accomplished are determined. The energy characteristics of single- and double-segment permeable thermoelements are calculated under optimal operating conditions for different values of heat carrier temperatures. It is shown that the efficiency of a permeable thermoelement depends on the geometry of legs (the height, the diameter and number of channels) and reaches maximum value of 4 % and 7 % for single- and double-segment variants, respectively.

Key words: computer design, permeable structures, heat recuperators, efficiency.

Introduction

In recent decade, due to growing demand for energy resources, increasing attention has been drawn to the recovery of heat from industry and internal combustion engines via thermoelectricity. The temperature level of such heat sources reaches 700 to 800 K. However, the constraining factor for a wide introduction of thermoelectric recuperators is insufficiently high efficiency of the existing thermoelectric materials. Moreover, the overwhelming majority of thermoelectric materials used nowadays for creation of thermoelectric converters include difficult to obtain and toxic components. With this consideration in mind, development and research on high-performance, cheap, environmentally safe thermoelectric materials and power converters on their basis is a relevant task.

One of the promising methods for efficiency improvement of thermoelectric converters and expansion of their possible practical implementation is to use materials based on *Mg* and *Mn* silicides which meet a number of requirements: low-cost initial components, high mechanical strength and, particularly, environmental safety.

Analysis of known investigations shows that the efficiency of thermoelectric modules made of homogeneous materials based on doped *n*-*Mg-Si* and *p*-*Mn-Si* solid solutions at hot side temperature 773K and cold side temperature 320 K is at a level of ~ 4 % [1]. Through use of double-segment structures based on *Mg* and *Mn* silicides the efficiency of modules is increased by a factor of 1.3 to 1.5. In [1] it is shown that the best efficiency values should be expected for *n*-type $Mg_2(Si_{0.3}Sn_{0.7})_{1-x}Sb_x$ and *p*-type $Mn(Al_xSi_{1-x})_{1.8}$ materials.

At the same time, studies on thermoelements where heat inlet and outlet takes place not only through the junction surfaces, but also due to the use of developed heat exchange surface in the bulk of thermoelement legs material have aroused heightened interest of late [2]. In such cases, thermoelements are created that are permeable to gas or liquid fluxes which allows improving the efficiency of thermoelectric energy conversion by 30 % already for the existing low-temperature generator materials based on Bi_2Te_3 [3]. Studies on such permeable thermoelements of promising

materials based on *Mg* and *Mn* silicides have not been performed.

The purpose of this work is calculation and study of the efficiency of permeable generator thermoelements made of optimal materials based on *Mg* and *Mn* silicides.

Physical model and its mathematical description

A physical model of a permeable thermoelement in electric energy generation mode is represented in Fig. 1. The thermoelement is composed of *n*- and *p*-type legs whose physical properties are temperature dependent. Heat input takes place by passing heat carrier along the leg through channels (pores). Each leg consists of N_n and N_p segments, respectively, with connection contact resistance r_0 . The lateral surfaces of legs are adiabatically isolated, heat carrier temperature at input to thermoelement T_m is assigned. Cold junction temperature T_c is thermostated.

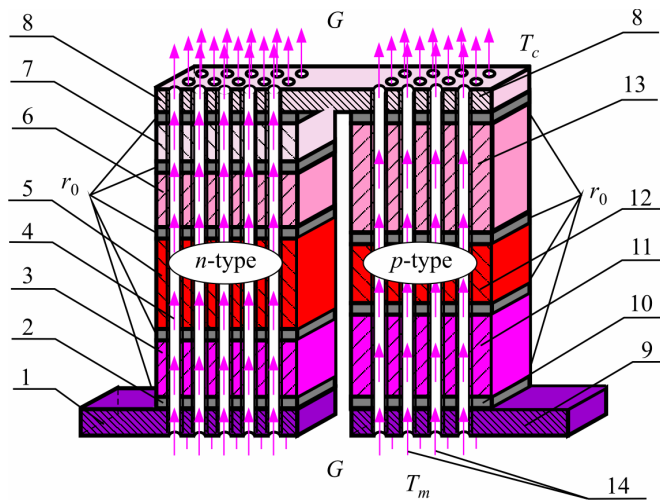


Fig. 1. Physical model of a permeable segmented thermoelement 1, 8, 9 – connecting plates; 2, 10 – connecting layers; 3, 5, 6, 7 – segments (sections) of *n*-type leg; 4 – heat carrier flux; 11, 12, 13 – segments (sections) of *p*-type leg; 14 – high thermally conductive dielectric.

A system of differential equations that describes the distribution of temperatures and heat fluxes in the steady-state one-dimensional case, in the infinitely small part dx of each k -th segment of *n*- and *p*-type legs, in dimensionless coordinates is of the form [3]:

$$\left. \begin{aligned} \frac{dT}{dx} &= -\frac{\alpha_k j}{\kappa_k} T - \frac{j}{\kappa_k} q, \\ \frac{dq}{dx} &= \frac{\alpha_k^2 j}{\kappa_k} T + \frac{\alpha_k j}{\kappa_k} q + j \rho_k + \frac{\alpha_T \Pi_K^1 N_k l_k^2}{(S - S_k) j} (t - T), \\ \frac{dt}{dx} &= \frac{\alpha_T \Pi_K^1 N_k l_k}{G c_P} (t - T), \end{aligned} \right\}_{n,p} \quad \begin{array}{l} k = 1, \dots, N_{n,p} \\ x_{k-1} \leq x \leq x_k \end{array} \quad (1)$$

where Π_K^1 is channel perimeter; N_k is the number of channels; S_k is cross-sectional area of all channels; S is cross-section of leg together with channels; l_k – height of k -th segment of leg; G is heat carrier flow rate in the channels; c_P is specific heat of heat carrier; t is heat carrier temperature at point x ; T is leg temperature at point x ; α_T is heat transfer coefficient; α , κ , ρ are the Seebeck coefficient, thermal conductivity and resistivity of leg material.

Specific heat fluxes q and reduced density of electric current j are determined by the relations:

$$q = \frac{Q}{I}, \quad j = \frac{Il}{S}, \quad (2)$$

where Q is power of heat flux that passes through thermoelement leg; I is electric current; $S_{n,p}$ is cross-sectional area of legs of n - and p -type thermoelement.

The boundary conditions necessary for solving (1) with regard to the Joule-Lenz heat release due to contact resistance r_0 at points of connection of leg segments are formulated in the form:

$$\begin{aligned} T_{n,p}(0) &= T_C, & t_{n,p}(1) &= T_m, & q_{n,p}(1) &= 0, \\ T_{n,p}(x_k^+) &= T_{n,p}(x_k^-), & q_{n,p}(x_k^+) &= q_{n,p}(x_k^-) + \frac{r_0}{S_{n,p}} I, \end{aligned} \quad (3)$$

where indices "−" and "+" denote the values of functions immediately to the left and right of the joint between x_k segments; $k = 1, \dots, N$ is the index that determines the number of leg segment.

In the case of search for optimal values of doping impurities that determine carrier concentrations in leg segments, it is necessary to assign the dependences of material parameters α , κ , ρ on temperature and concentration of carriers (or impurities) C_k : $\alpha_k = \alpha_k(C_k, T)$, $\rho_k = \rho_k(C_k, T)$, $\kappa_k = \kappa_k(C_k, T)$.

The goal of designing a permeable segmented generator thermoelement is to determine such matched parameters (reduced current density j in the legs, heat carrier losses in channels G , concentration of doping impurities in materials of each segment C_k), whereby thermoelement efficiency reaches its maximum value.

The efficiency will be found through the ratio between the electric power P generated by thermoelement and the change in heat carrier enthalpy:

$$\eta = \frac{P}{\sum_{n,p} G c_p (T_m - T_C)}. \quad (4)$$

Efficiency maximum can be conveniently reduced to achieve functional minimum:

$$J = \ln \left[\sum_{n,p} \{G c_p (T_m - T_C)\} \right] - \ln \left[\sum_{n,p} \left\{ G c_p (T_m - t(0)) + q(0) \frac{j(S - S_K)}{l} - I \left(\frac{r_0}{S_n} + \frac{r_0}{S_p} \right) \right\} \right]. \quad (5)$$

The problem was solved using the Pontryagin maximum principle [4] giving the necessary optimality conditions:

1) optimal values of specific current density in thermoelement legs j must satisfy the equalities

$$-\left[\frac{\partial J}{\partial j} \right]_{n,p} + \sum_{n,p} \int_0^1 \left[\psi_1^k \frac{\partial f_1^k}{\partial j_k} + \psi_2^k \frac{\partial f_2^k}{\partial j_k} + \psi_3^k \frac{\partial f_3^k}{\partial j_k} \right]_{n,p} dx = 0, \quad (6)$$

where $(f_1^k, f_2^k, f_3^k)_{n,p}$ are right-hand sides of equations (1); $\psi = (\psi_1^k, \psi_2^k, \psi_3^k)_{n,p}$ is vector function of pulses [3, 4] found from solving an auxiliary system of differential equations

$$\left. \begin{aligned} \frac{d\psi_1}{dx} &= \frac{\alpha_k j_k}{\kappa_k} R_1 \psi_1 - \left(\frac{\alpha_k j_k}{\kappa_k} R_2 - \frac{\alpha_e l_k}{(S - S_K) j_k} \right) \psi_2 + \frac{\alpha_T \Pi_K^1 N_K}{G c_p} \psi_3, \\ \frac{d\psi_2}{dx} &= \frac{j_k}{\kappa_k} \psi_1 - \frac{\alpha_k j_k}{\kappa_k} \psi_2, \\ \frac{d\psi_3}{dx} &= -\frac{\alpha_T \Pi_K^1 N_K l_k}{(S - S_K) j_k} \psi_2 - \frac{\alpha_T \Pi_K^1 N_K}{G c_p} \psi_3, \end{aligned} \right\}_{n,p} \quad (7)$$

$$\left. \begin{aligned} R_1 &= 1 + \frac{d \ln \alpha}{dT} T - \frac{d \ln \kappa}{dT} \left(T + \frac{q}{\alpha} \right), \\ R_2 &= R_1 + \frac{\kappa}{\alpha^2 \sigma} \frac{d \ln \sigma}{dT} + \frac{d \ln \kappa}{dT} \left(T + \frac{q}{\alpha} \right). \end{aligned} \right\}_{n,p}$$

where

With the boundary conditions

$$\begin{aligned} \psi_1^{n,p}(1) &= 0, \\ \psi_2^{n,p}(0) &= \frac{j(S - S_K)}{\sum_{n,p} \left\{ Gc_P(T_m - t(0)) + q(0) \frac{j(S - S_K)}{l} - I \left(\frac{r_0}{S_n} + \frac{r_0}{S_p} \right) \right\}}, \\ \psi_3^{n,p}(0) &= \frac{Gc_P}{\sum_{n,p} \left\{ Gc_P(T_m - t(0)) + q(0) \frac{j(S - S_K)}{l} - I \left(\frac{r_0}{S_n} + \frac{r_0}{S_p} \right) \right\}}. \end{aligned} \quad (8)$$

2) optimal values of heat carrier flow rate G in the channels

$$-\left[\frac{\partial J}{\partial G} \right]_{n,p} + \sum_{n,p} \int_0^1 \left[\psi_1^k \frac{\partial f_1^k}{\partial G} + \psi_2^k \frac{\partial f_2^k}{\partial G} + \psi_3^k \frac{\partial f_3^k}{\partial G} \right]_{n,p} dx = 0. \quad (9)$$

3) optimal values of doping impurities in material of each segment C_k are found from the ratios

$$\int_0^1 \left[\psi_1^k \frac{\partial f_1^k}{\partial C_k} + \psi_2^k \frac{\partial f_2^k}{\partial C_k} + \psi_3^k \frac{\partial f_3^k}{\partial C_k} \right]_{n,p} dx = 0, \quad k = 1, \dots, N_{n,p}. \quad (10)$$

In case of thermoelement design for fixed materials in the segments the optimality conditions (10) are disregarded.

Based on the obtained relations, using successive approximation method, the Runge-Kutta numerical method for solving systems of differential equations (1) and (7) with the boundary conditions (3) and (8), the Newton method for solving systems of integral-differential equations (6), (9), (10), a computer program was developed for the design of permeable segmented thermoelement. The results of computer studies are given below.

Results of computer studies of the energy characteristics of permeable segmented generator thermoelement based on Mg and Mn silicides

Fabrication techniques of materials based on magnesium and manganese silicides and the results of experimental research on their thermoelectric properties are described in a number of scientific papers [5-12]. Analysis has revealed that with regard to the figure of merit value, the most advisable materials for creation of generator thermoelements are as follows:

– $Mg_2(Si_{0.3}Sn_{0.7})_{1-x}Sb_x$ ($0 \leq x \leq 0.04$) for n -type legs which is obtained in the course of a two-stage solid-phase reaction in combination with spark plasma sintering [6]. Maximum figure of merit of this antimony-doped silicide is $ZT \approx 1.0$ at 640 K for the composition of $x = 0.025$.

– $Mn(Al_xSi_{1-x})_{1.80}$ ($0 \leq x \leq 0.003$) for p -type legs which is obtained by induction melting with further hot pressing [7]. Maximum figure of merit of such aluminum-doped manganese silicide is $ZT \approx 0.65$ at 850 K for the composition of $x = 0.0015$.

The above materials were selected for computer investigations of the energy characteristics of permeable thermoelements. The experimental dependences of their parameters α , κ , σ were approximated in the form of polynomial dependences on temperature T and doping parameter C (doping with antimony silicide ($0 \leq x \leq 0.04$) for n -type leg and doping with aluminum ($0 \leq x \leq 0.003$) for p -type).

Calculation of permeable segmented thermoelement was performed under the following conditions: heat exchange coefficient $\alpha_T = 0.01 \text{ W/cm}^2\cdot\text{K}$, cross-sectional area of leg together with channels $S = 1 \text{ cm}^2$, contact resistance at points of leg segments connection $r_0 = 5 \cdot 10^{-6} \Omega \cdot \text{cm}^2$.

Optimal parameters of thermoelement were found, and the energy characteristics of double-segment permeable thermoelement with channel diameter $d_k = 0.1 \text{ cm}$, the number of channels $N_k = 25$ pcs per 1 cm^2 depending on the height of legs are listed in Table 1. The calculated results are given for the case when heat carrier temperature at thermoelement inlet is $T_m = 900 \text{ K}$, and cold junction temperature is $T_c = 300 \text{ K}$. It is seen that hot junction temperature of thermoelement under optimal operating conditions is $T_n(1) = 495 \text{ K}$.

Table 1

Optimal parameters and energy characteristics of a double-segment permeable thermoelement based on Mg and Mn silicides

| l , cm | EMF _{max} , | $t_n(0)$, K | $T_n(1)$, K | P , W | G_{opt} , g·cm/s | j_{opt} , A/cm | $C_1^n_{opt}$ | $C_2^n_{opt}$ | $C_1^p_{opt}$ | $C_2^p_{opt}$ |
|-------------|----------------------|-----------------|-----------------|------------|-----------------------|---------------------|---------------|---------------|---------------|---------------|
| 0.6 | 0.019 | 373.4 | 391.0 | 0.339 | 0.0150 | 4.29 | 0.00409 | 0.0229 | 0.00159 | 0.00187 |
| 0.7 | 0.023 | 371.3 | 409.0 | 0.426 | 0.0156 | 5.08 | 0.00394 | 0.0229 | 0.00161 | 0.00188 |
| 0.8 | 0.026 | 369.2 | 424.9 | 0.503 | 0.0158 | 5.82 | 0.00374 | 0.0229 | 0.00164 | 0.00189 |
| 0.9 | 0.030 | 366.4 | 438.3 | 0.565 | 0.0158 | 6.47 | 0.00352 | 0.0229 | 0.00166 | 0.00190 |
| 1.0 | 0.033 | 363.2 | 449.3 | 0.612 | 0.0157 | 7.03 | 0.00328 | 0.0228 | 0.00169 | 0.00190 |
| 1.1 | 0.035 | 359.6 | 458.3 | 0.647 | 0.0153 | 7.51 | 0.00303 | 0.0228 | 0.00171 | 0.00191 |
| 1.2 | 0.037 | 356.0 | 465.5 | 0.670 | 0.0149 | 7.93 | 0.00278 | 0.0228 | 0.00173 | 0.00191 |
| 1.3 | 0.039 | 352.3 | 471.3 | 0.685 | 0.0145 | 8.30 | 0.00254 | 0.0228 | 0.00175 | 0.00192 |
| 1.4 | 0.041 | 348.8 | 476.0 | 0.692 | 0.0141 | 8.62 | 0.00231 | 0.0228 | 0.00177 | 0.00192 |
| 1.5 | 0.043 | 345.4 | 479.7 | 0.695 | 0.0136 | 8.91 | 0.00209 | 0.0228 | 0.00178 | 0.00193 |
| 1.6 | 0.044 | 342.5 | 482.9 | 0.697 | 0.0132 | 9.26 | 0.00185 | 0.0228 | 0.00180 | 0.00194 |
| 1.7 | 0.045 | 339.6 | 485.4 | 0.693 | 0.0128 | 9.51 | 0.00164 | 0.0228 | 0.00182 | 0.00194 |
| 1.8 | 0.046 | 336.9 | 487.5 | 0.687 | 0.0124 | 9.73 | 0.00145 | 0.0228 | 0.00183 | 0.00194 |
| 1.9 | 0.047 | 334.3 | 489.1 | 0.678 | 0.0120 | 9.91 | 0.00128 | 0.0228 | 0.00185 | 0.00195 |
| 2.0 | 0.048 | 332.0 | 490.4 | 0.668 | 0.0116 | 10.08 | 0.00112 | 0.0228 | 0.00186 | 0.00195 |
| 2.1 | 0.049 | 329.8 | 491.5 | 0.657 | 0.0113 | 10.23 | 0.00097 | 0.0228 | 0.00187 | 0.00196 |
| 2.2 | 0.049 | 327.8 | 492.4 | 0.645 | 0.0109 | 10.36 | 0.00083 | 0.0228 | 0.00188 | 0.00196 |
| 2.3 | 0.050 | 326.0 | 493.2 | 0.633 | 0.0106 | 10.48 | 0.00070 | 0.0228 | 0.00189 | 0.00196 |
| 2.4 | 0.050 | 324.3 | 493.8 | 0.620 | 0.0103 | 10.59 | 0.00058 | 0.0228 | 0.00190 | 0.00196 |
| 2.5 | 0.051 | 322.8 | 494.3 | 0.608 | 0.0100 | 10.69 | 0.00047 | 0.0228 | 0.00191 | 0.00197 |
| 2.6 | 0.051 | 321.4 | 494.7 | 0.596 | 0.0097 | 10.78 | 0.00037 | 0.0228 | 0.00192 | 0.00197 |
| 2.7 | 0.052 | 320.1 | 495.0 | 0.583 | 0.0094 | 10.86 | 0.00027 | 0.0228 | 0.00192 | 0.00197 |
| 2.8 | 0.052 | 318.9 | 495.3 | 0.571 | 0.0091 | 10.94 | 0.00019 | 0.0228 | 0.00193 | 0.00197 |
| 2.9 | 0.052 | 317.8 | 495.6 | 0.559 | 0.0089 | 11.01 | 0.00010 | 0.0228 | 0.00194 | 0.00198 |
| 3.0 | 0.053 | 316.8 | 495.8 | 0.547 | 0.0087 | 11.07 | 0.00003 | 0.0228 | 0.00194 | 0.00198 |

In so doing, heat carrier temperature at thermoelement outlet approaches cold junction temperature and is at a level of $t_n(0) = 317$ K, that is, heat carrier enthalpy is reduced by the value of temperature difference $(900 - 330) = 570$ K, which approaches the available change of temperatures $(T_m - T_c) = 600$ K. This testifies to a more complete utilization of heat carrier thermal energy as compared to classical thermocouple elements, where only half the available temperature difference is used beneficially [2].

Fig. 2 shows a dependence of maximum efficiency η and the respective specific electric power W of permeable segmented generator thermoelement at optimal values of j , G and doping parameter C in leg segments on the general height of legs l . It is seen that with increase in leg height, the efficiency grows and reaches saturation near the value of 5.5 %, and the respective specific power P has an extremum at the leg height $l \sim 1.5$ cm.

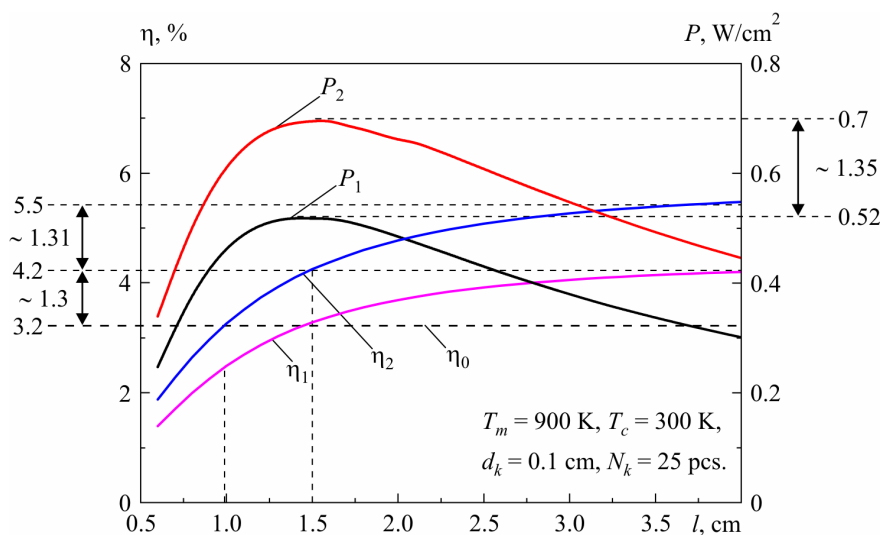


Fig. 2. Dependence of the energy characteristics of a permeable segmented thermoelement based on Mg and Mn silicides on leg length l . 1 – single-segment permeable thermoelements; 2 – double-segment permeable thermoelements.

At such height (1.5 cm) maximum efficiency value (for a single-segment permeable thermoelement) is about 3.2 %, which corresponds to the efficiency of classical thermocouple thermoelement ($\eta_0 = 3.2$ %) under similar operating conditions. In so doing, the specific power value does not exceed $0.52 \text{ W}/\text{cm}^2$ for a single-segment leg and $0.7 \text{ W}/\text{cm}^2$ for a double-segment leg.

Calculation results show that with increase in the number of leg segments, there is saturation both in the value of specific power and the efficiency. Hence, the reasonable number of leg segments makes 2 – 3 pcs. Further build up of segments does not result in considerable improvement of energy conversion characteristics which is also typical of classical segmented thermoelements [13].

Results of research on the dependence of the energy characteristics of a permeable segmented generator thermoelement on channel diameter d_k for single- (index 1) and double-segment legs (index 2) under conditions of optimal values of j , G and concentrations of doping impurities in leg segments are given in Fig. 3.

It is seen that increase in channel diameter improves energy conversion efficiency. In so doing, the electric power in maximum efficiency mode has an extremum in the case of $d_k = 0.14$ cm, whereby the efficiency is 3.2 % for a single-segment thermoelement and 4 % for a double-segment thermoelement. The results obtained show that for practical applications the reasonable channel diameter of a permeable segmented thermoelement will lie within 1 to 2 cm.

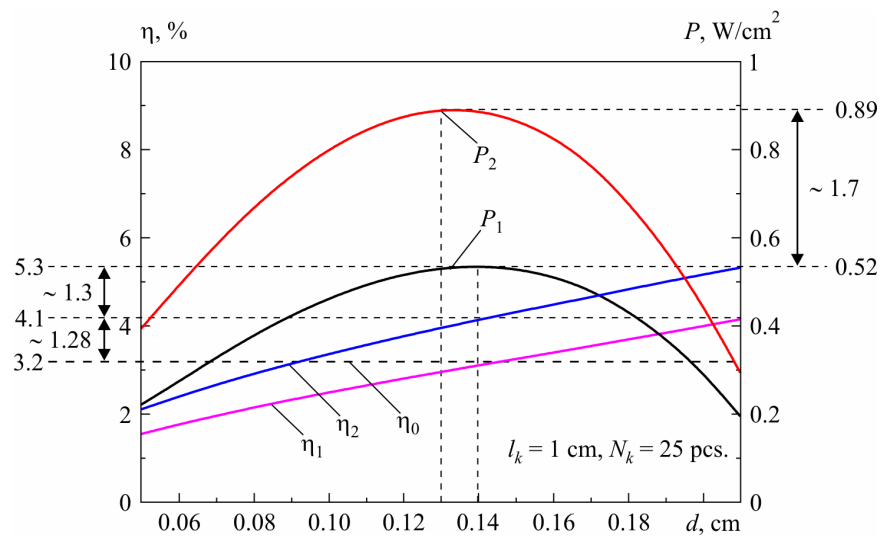


Fig. 3. Dependence of the energy characteristics of a permeable segmented thermoelement on channel diameter d_k . 1 – single-segment permeable thermoelements; 2 – double-segment permeable thermoelements.

The effect of the number of channels N_k on the energy characteristics of a permeable thermoelement under conditions of optimal j , G and C_k for different number of leg segments N is shown in Fig. 4.

It is evident that the efficiency grows with increase in the number of channels, reaching the saturation. In so doing, the specific electric power has a maximum observed at 13 channels per 1 cm². So, the rational number of channels per unit area will be within 10 to 24 pcs per 1 cm². Considerable efficiency increase depending on the number of segments of thermoelement legs N is also observed only for the variant of using 2 segments. Further increase in the number of segments does not result in essential efficiency and specific power increase.

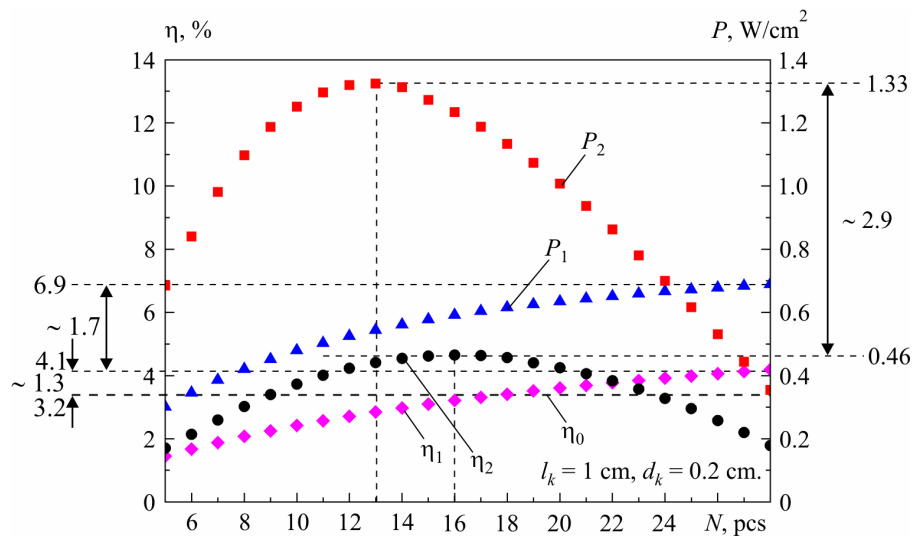


Fig. 4. Dependence of the energy characteristics of a permeable segmented thermoelement on the number of channels N_k . 1 – single-segment permeable thermoelements; 2 – double-segment permeable thermoelements.

Comparison of the efficiency of permeable thermoelement to that of classical thermoelement η_0 under similar operating conditions testifies to possible increase of energy conversion efficiency by 30 to 40 %.

Conclusions

1. Procedure for calculation and design of a permeable generator thermoelement of segmented materials based on *Mg* and *Mn* silicides is represented.
2. The effect of structural parameters (the diameter and number of channels, the height of legs and the number of segments) under optimal efficiency operating conditions on the basic energy conversion characteristics is determined. The reasonable values of such parameters are found, which allows finding the necessary material science and technological requirements for the development of a permeable thermoelement.
3. It is shown that with the use of materials based on *Mg* and *Mn* silicides for a permeable segmented thermoelement at the initial heat carrier temperature 900 K and thermostated cold junctions at a level of 300 K, the reasonable number of leg segments is 2 pcs. Comparison of a permeable thermoelements in terms of thermodynamic energy conversion efficiency to conventional thermoelements has shown the possibility of energy conversion efficiency increase by 30 to 40 %.

References

1. V.R. Bilinsky-Slotylo, L.M. Vikhor, and V.Ya. Mykhailovsky, Design of Thermoelectric Generator Modules from *Mg* and *Mn* Silicide Based Materials, *J. Thermoelectricity* **1**, 60 – 66 (2013).
2. L.I. Anatychuk, R.G. Cherkez, Permeable Thermoelement in Electric Energy Generation Mode, *J. Thermoelectricity* **2**, 35 – 46 (2003).
3. L.I. Anatychuk, R.G. Cherkez, Permeable Sectional Thermoelement in Electric Energy Generation Mode, *J. Thermoelectricity* **3**, 5 – 12 (2010).
4. L.S. Pontryagin, V.G. Boltyansky, R.V. Gamkrelidze, and E.F. Mischenko, *Mathematical Theory of Optimal Processes* (Moscow: Nauka, 1976), 392 p.
5. Zh. Du, T. Zhu, and X. Zhao, Enhanced Thermoelectric Properties of $Mg_2Si_{0.58}Sn_{0.42}$ Compounds by *Bi* Doping, *Materials Letters* **66** (1), 76 (2012).
6. W. Liu, Q. Zhang, X. Tang X et al., Thermoelectric Properties of *Sb*-Doped $Mg_2Si_{0.3}Sn_{0.7}$, *Journal of Electronic Materials* **40** (5), 1062 (2011).
7. W. Luo, H. Li, F. Fu et al., Improved Thermoelectric Properties of *Al*-Doped Higher Manganese Silicide Prepared by a Rapid Solidification Method, *Journal of Electronic Materials* **40** (5), 1233 (2011).
8. A.J. Zhou, T.J. Zhu, X.B. Zhao et al., Improved Thermoelectric Performance of Higher Manganese Silicides with *Ge* Additions, *Journal of Electronic Materials* **39** (9), 2002 (2010).
9. M.J. Yang, L.M. Zhang, L.Q. Han et al., Simple Fabrication of Mg_2Si Thermoelectric Generator by Spark Plasma Sintering, *Indian Journal of Engineering and Materials Sciences* **16**, 277 (2009).
10. T. Sakamoto, T. Iida, A. Matsumoto et al., Thermoelectric Characteristics of a Commercialized Mg_2Si Source Doped with *Al*, *Bi*, *Ag*, and *Cu*, *Journal of Electronic Materials* **39** (9), 1708 (2010).
11. T. Sakamoto, T. Iida, Sh. Kuroasaki et al., Thermoelectric Behavior of *Sb*- and *Al*-Doped *n*-Type Mg_2Si Device Under Large Temperature Differences, *Journal of Electronic Materials* **40** (5), 629 (2011).
12. R. Song, Y. Liu, and T. Aizawa, Solid State Synthesis and Thermoelectric Properties of *Mg-Si-Ge* System, *Journal of Materials Science & Technology* **21** (5), 618 (2005).
13. L.I. Anatychuk, L.N. Vikhor, Generator Modules of Segmented Thermoelements, *Energy Conversion and Management* **50** (9), 2366 – 2372 (2009).

Submitted 20.12.2013.